Bearing Capacity of Triangular Shell Foundations Adjacent to the Reinforced Sandy Slopes

Seyed Ali Ghaffari[1], Amir Hamidi[*1],

Gholamhosein Tavakoli Mehrjardi[1]

1. School of Engineering, Kharazmi University, Tehran,

Abstract

This paper investigates the response of triangular shell strip footings situated on the sandy slope. A series of reduced-scale plate load tests were conducted to cover different parameters including three shell footing types with different apex angles in addition to a flat footing, four different distances for strip footings from the crest of the slope namely "edge distance" and reinforcement status (unreinforced and geotextile-reinforced statuses). Bearing capacity of shell footings adjacent to crest of the slope, bearing capacity ratio, shell efficiency factor, influence of apex angle on settlement of footings and the mechanism of slope failure are discussed and evaluated. Also, empirical equations for determination of the maximum bearing capacity of triangular shell strip footings are suggested. As a whole, it has been observed that decrease of shell's apex angle as good as increase of edge distance could significantly improve the bearing capacity. However, as the edge distance increases, the effect of apex angle on the bearing capacity got decreased. Also, it was found out that the beneficial effect of

*Corresponding author   hamidi@khu.ac.ir

reinforcement on the bearing capacity decreased with increase of the edge distance. Furthermore, the efficiency of shell footings on bearing capacity was attenuated in reinforced slopes compared to the unreinforced status.

Keywords: Soil-geosynthetic interaction; Geotextiles; shells; foundations; slope stabilization.

Introduction

Due to the important role of foundations on the stability of structures, a number of researchers investigated application of safer and more economical footings like shell foundations. Shells are thin-walled structures which obtain the stability and bearing capacity from their specified shape. This characteristic enables them to create maximum structural efficiency with minimum materials [1-4]. From geotechnical point of view, the specific performance of shell footings has been directly related to different shapes including conical, pyramidal and triangular shell strip footings [4-7].

The bearing capacity and settlement of triangular shell strip footings located on the sand has been experimentally investigated by a number of researchers [8-9]. Their studies have showed that bearing capacity and settlement characteristics of shell footings were significantly improved compared to the flat one. Also, the bearing capacity of triangular shell strip footings on unreinforced and geotextile-reinforced sand has been studied using experimental models and the effects of soil compaction and geotextile reinforcement beneath the foundation on the maximum bearing capacity of shell footing has been evaluated [10-11]. These studies

confirmed increase of bearing capacity of shell footings with decrease in apex angle. Moreover, decrease in bearing capacity was observed due to increase in depth of geotextile layers. Furthermore, the investigations showed that the failure wedge of reinforced shell foundation was formed deeper than conventional flat ones.

In many cases, deficiency of land in urban areas and replacement of the buildings and retaining walls near river banks have forced construction operations at the vicinity of slopes which proves the need for investigation of the safer and more economical footings. The benefits of shell footings on extension of failure wedge into the depth of soil embankment impressed the authors to investigate the response of this foundation system at the vicinity of slopes. A number of researchers investigated performance of conventional flat footings situated near the unreinforced and reinforced sandy slopes [12-21]. Results of previous studies indicate that the maximum bearing capacity of flat footing and their settlement characteristics can be improved significantly by using reinforcement layers considering the effects of edge distance.

As a whole, review of the studies reveals lack of technical reports on the performance of shell footings adjacent to the reinforced and unreinforced slopes. For this purpose, in the present study, a series of reduced-scale plate load tests have been conducted to investigate the behavior of triangular shell strip footings adjacent to the sandy slopes. For the sake of comparison, similar tests have been carried out to investigate the performance of shell footings located on the flat ground.

Test Materials

Backfill Soil

In this study, to construct the slope, uniform and clean quartz beach sand, namely "Babolsar sand" (extracted from Babolsar's shores located at North of Iran), was used as backfill materials. Figure 1 shows the grain size distribution of this sand. Also, the physical properties of the soil, which is classified as SP in Unified Soil Classification System, are tabulated in Table 1 [22].

Geotextile

The geotextiles which are expanded over the slope backfills were made of high strength woven polyester manufactured from high tenacity and high molecular weight multifilament polyester yarns. The mechanical properties of the geotextiles used in this study are depicted in Table 2.
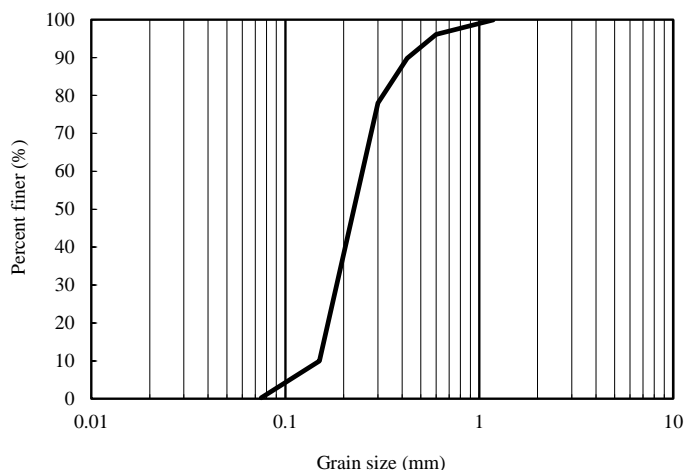

Figure 1. Grain size distribution curve for Babolsar sand

Footing Model

According to Figure 2, three types of triangular shell footings namely ''shell footing'' and one type of strip footing namely ''simple footing'' were used in the present investigation. The dimensions of footings in plane were 100 mm in width and 640 mm in length, simulating the plane strain conditions. The apex angles of 60°, 90°, 120° (shell footing) and 180° (simple footing) have been chosen to examine the response of the foundation system. These values can be representative of a practical range for construction purposes [9]. All the other dimensions of footings' geometry were kept the same. As shown in Figs. 2(a-c), the height of footings is the same and equals to 50 mm. For the apex angle of 60° at Figure 2 (d), the thickness of top portion increased to 57 mm to avoid bending or breakage of the model during loading. Furthermore, for the metallic footings used in present study, the aspect ratio is an important parameter which controls buckling of foundations during axial loading. The height and width of all footings were considered the same to provide similar aspect ratio (h/B=50/100=0.5).

The footing models were made of high-quality aluminum alloy (Type 6061), using the Computer Numerical Control method (CNC). Aluminum shell foundations have been previously used in experimental studies on shell foundations by other researchers [6]. In fact, Aluminum is a deformable and light metal which can be simply trimmed to construct small scale shell foundations of different angles and shapes. Each model was fabricated from shaving an ingot of alloy to obtain a uniform structure without nodes and hinges. Overall view of four footings is shown in Figure 3.
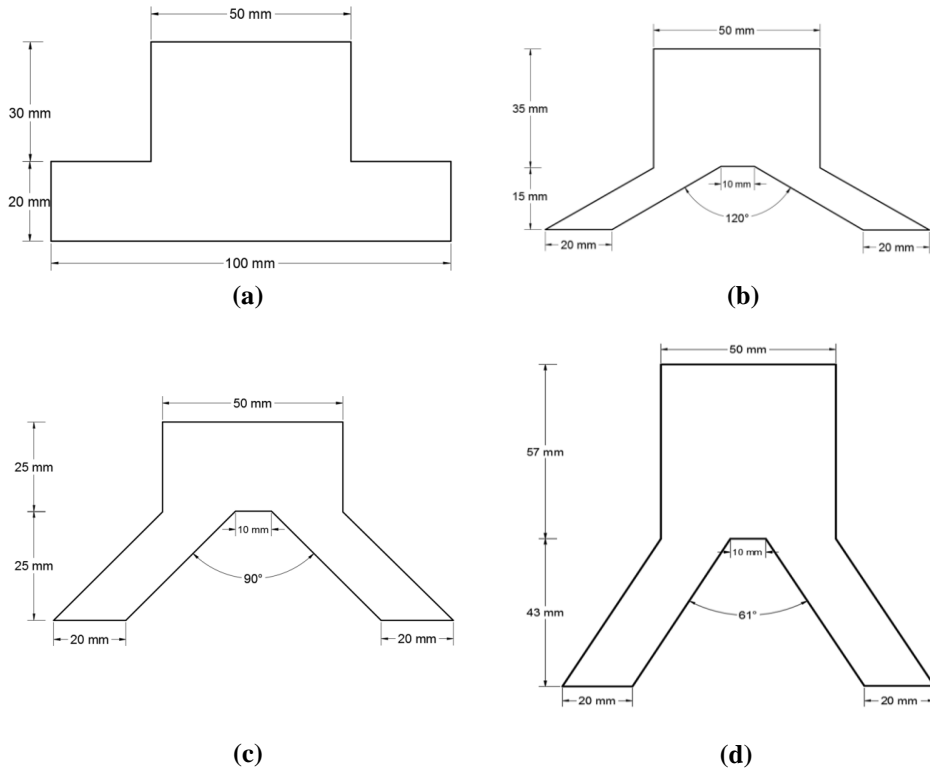
(a)

(b)

(c)   **(d)**

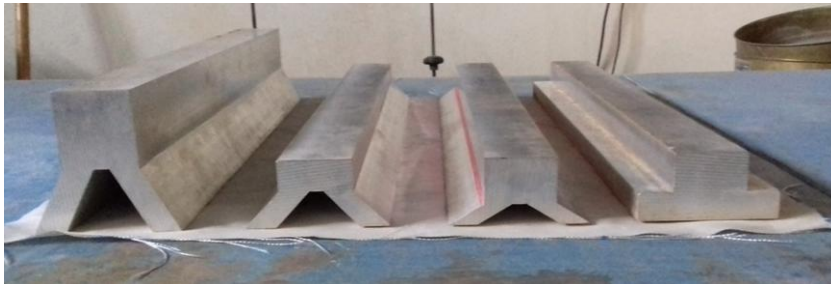**Figure 2. Geometrical configuration of footings**

Figure 3. Overall view of the footings

Test Setup, Instrumentation and Test Procedures

In this study, a test box with steel frame was utilized to perform all the tests. Figure 4(a) shows schematic representation of the test

box and other equipment. Dimensions of the box were 1200 mm in length, 700 mm in width and 700 mm in height. Three sidewalls of the test box were made of 20 mm-thick fiberglass to observe induced failure surfaces during testing. Sidewalls were supported by two steel columns. Also, a steel plate was used in the floor to ensure rigidity of the tank. A number of researchers have observed that the failure zone in the footing bed extends over a distance of about 2 to 2.5 times of the footing width and away from footing center which has been also considered in determination of box dimensions in present study [23-25]. The box length is 1200 mm and the ratio of box to footing width is 12, which guarantees zero lateral deflection of the sides during loading and any interference of the failure surface with the box.

In all tests, the embankment was constructed in two 150 mm layers and one 100 mm layer to reach the 400 mm height. The unit weight of the poured sand was determined based on the relative density of 70%. The maximum and minimum unit weights of sand were determined according to ASTM standards [26-27]. Then, the required weight of soil was determined according to the volume of the box. Each layer of soil was compacted to the associated height of box to ensure obtaining the desired relative density. Compaction of each layer was performed by a vibratory compactor to reach relative density of 70%, having moisture content of 4.5%. Then, the embankment was trimmed to reach sloped backfill with an angle of $45°$ as shown in Figure 4(b). Indeed, this is the representative slope angle at which the embankment remains stable under its weight. By conducting some triaxial tests on Babolsar sand at the mentioned

relative density in different confining pressures, friction angle of the soil was determined equal to $41°$. It was tried to keep the moisture content of the backfill constant as much as possible. It should also be noted that the embedment depth has been considered equal to zero for all footings in this study as shown in Figure 4(b).

It has been mentioned by previous researchers that the optimum depth of planar reinforcements is 1-1.5 times of loading plate width [28-30]. Therefore, two layers of geotextile reinforcement were implemented in present study, as can be seen in Figure 4(b). Herein, the upper and lower geotextile layers were named as the first and second layers, respectively. The embedment depth of first layer (u) was considered 0.5B (50 mm in this study) as suggested by previous studies [31]. Also, the distance between reinforcement layers (h) was selected as 0.7B (70 mm in present study) based on other researches [15]. A number of researchers have proposed that regardless of the footing distance from the slope's crest, enough length of reinforcement for fine sands is 6 times of footing width that is 600 mm in current research [19].
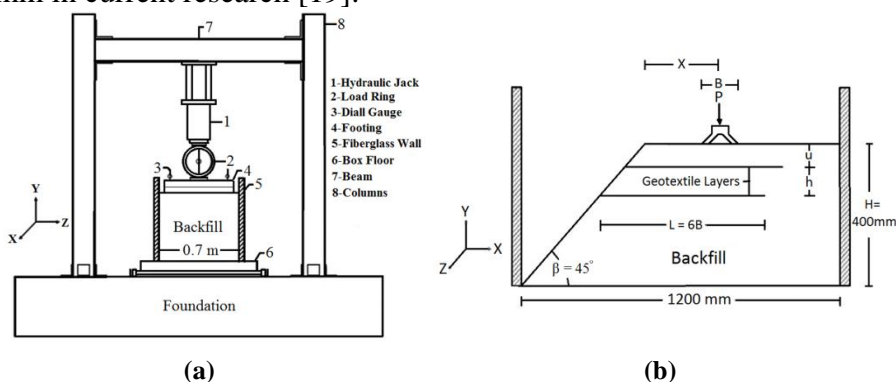

(a)   (b)

Figure 4. schematic representation of (a) test setup, (b) slope and shell footing

In practice, shell foundations are constructed by either of cast-in-place or precast methods. In the cast-in-place method, at first, the soil is cut to fit the core beneath the shell foundation and then, the subgrade is grouted to obtain a smooth surface. After that, shell footing made of reinforced concrete is constructed. There are two construction strategies for the precast method. The precast shell can be transferred from factory and placed upon the cutting edge at the same shape of the core and the gap between footing and soil would be filled with pressure-controlled grout.

At the second method, precast shell is placed on the flat subgrade and the gap between it and soil is filled by sand pouring thorough the holes placed on the precast foundation. The compaction of the core sand can be done using a small rotary vibrator.

The similarity between model tests and field conditions is limited to the precast foundations prepared by the first method. After installation, the steel plate was slowly and horizontally pulled out to keep a full contact between the footing-soil components and slope backfill.

The monotonic loading system consists of a hand-operated hydraulic jack and pre-calibrated load ring, mounted on the footing that was located at specified distance from the slope edge. The hydraulic jack applied loading via a pre-calibrated load ring with a capacity of 5000kg and accuracy of ±0.01% of full range that was located between the loading shaft and footing. The loading was applied on a small plate welded at the centerline of the footing without any fixed connection. In order to control any possible

rocking or tilting of the footings, settlements were monitored using two dial gauges with an accuracy of 0.01% of full range (60 mm) located on opposite edges of the loading shell. The average value of recorded settlements was reported as the footing settlement at each loading step.

The load was applied with increments of 0.4kN and was maintained until the footing settlement reached to a constant value. However, in all the tests, monotonic loading was continued incrementally up to the maximum settlement of 0.25B, where B is width of the shell footing (100 mm in this study). Figure 5 shows a view of the model during loading and also the vibratory tamper used in compaction of the soil layers.

(a)   (b)

Figure 5. Vibratory tamper and test box during loading
(a) Vibratory tamper   (b) Loading frame and test box

Experimental Program

To investigate the influence of different parameters such as shell footing's apex angle, reinforcement status, and distance of footing

from slope's crest on the bearing capacity and settlement of the footings, a comprehensive testing program was established. In this regard, a total number of 40 small scale plate load tests were conducted.

Table 3 shows different studied variables including four different apex angles of the shell footing, reinforcement conditions (Re or Ur) and four different edge distances (distance of footing centerline to the slope's crest). Also, in order to compare the performance of shell footings situated on sloped and flat ground, a set of tests on flat backfill was performed in both unreinforced and reinforced conditions.

Results and Discussion

In this section, effects of different parameters such as soil reinforcement status, geometry of shell footing specified by apex angle, backfill geometry specified by flat and sloped conditions on the bearing capacity and settlement of foundation are discussed and evaluated. Also, failure mechanism of each system is comprehensively investigated. At the end, empirical equations are suggested for prediction of the bearing capacity of shell foundations based on the obtained test results.

Bearing Capacity of Foundations

Unreinforced Slope

Figure 6 illustrates the force-settlement curves of simple (apex angle, $i=180^{o}$) and shell footings (apex angle, $i=60, 90$ and 120°)

located on the unreinforced slopes at different edge distances. As it can be seen, for all footings, the largest value of bearing capacity belongs to the "flat" (no slope) state. In fact, the bearing capacity of foundation on the sloped backfill was highly decreased compared to that of the flat backfill due to the removing an effective part of resistant zone. The failure mode of the footings located on the flat ground was the local shear; however, a general shear mode of failure was observed for the foundations on the sloped backfill regardless of the edge distance.

Table 4 shows the values of applied force at failure, for foundation rested on unreinforced flat and sloped backfill with different edge distances. Depending on the edge distance, it can be concluded that the bearing capacity of foundations increased as the apex angle decreased. As it can be seen, for flat backfill, the bearing capacity of shell foundations was in the range of 8 to 18% more than the simple foundation, depending on the apex angle. It can be due to the fact that the shell footings extend the failure zone into the depth of foundation, tending to provision of more resisting force against failure. This is in agreement with experimental studies of other researchers [3, 9, 32].

In order to determine the amount of bearing capacity reduction due to the slope existence compared to the flat ground, the bearing capacity decrease factor in unreinforced status, $(BCD)_u$ is defined according to Eq. (1).
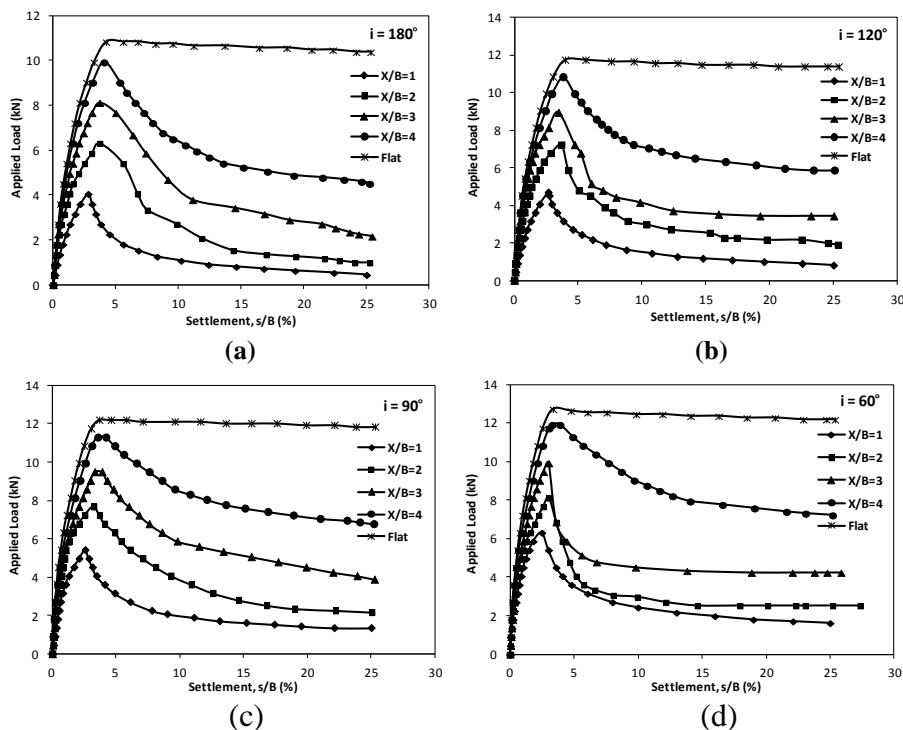
$$(BCD)_u = \frac{(Q_u)_f - (Q_u)_s}{(Q_u)_f} \tag{1}$$

Figure 6. Load-settlement response of unreinforced foundation on slope and flat backfills for (a) simple footing and shell footing with (b) i=120°, (c) i=90°, (d) i=60°.

$(Q_u)_f$ and $(Q_u)_s$ are the maximum bearing capacity of footings in flat and sloped backfills, respectively. As it is seen in Table 4, $(BCD)_u$ increased continuously as the edge distance decreased. Also, by comparing $(BCD)_u$ of shell footings with different apex angles, it is well understood that shell footing with apex angle of 60°, reflected the minimum amount of bearing capacity reduction. Conceivably, this kind of geometry could use the highest benefits from deeper failure mechanism, tending to postpone the instability. From the

obtained results, it can also be concluded that the ultimate bearing capacity of foundation in sloped backfill approaches to that of flat condition, if footings locate at the edge distances larger than 4B that is in the line with findings of other researchers, recommended the minimum safe edge distance of footing as 3.5B [19].

Reinforced Slope

Figure 7 depicts variations of applied force versus settlements of footings rested on the reinforced slope with different apex angles. As it can be seen, the settlement associated with the ultimate bearing load was smoothly increased as the apex angle of the shell footing became more acute, approaching that of the flat condition. In this regard, the rate of increase in ultimate bearing capacity for shell footing with apex angle of 60° compared the simple footing (i=180°) was 43% and 17% in sloped backfill (with an edge distance of 1B) and flat ground, respectively.

Table 5 shows the values of failure load for foundations rested on reinforced flat and sloped backfill with different edge distances. Comparing the presented results in Tables 4 and 5, it can be concluded that the rate of change in bearing capacity was in the range of 18 to 56% and 17 to 43% for unreinforced and reinforced backfills, respectively depending on the edge distance. This can be explained due to the fact that, contrary to the shell foundation system, the reinforcement layers prevented stress distribution into the soil depth and expanded the stress zone horizontally. As a result, the overall mutual effects resulted in debilitation of shell foundation efficiency. Also, as it can be seen, values of "BCD" in the reinforced

state are smaller than those in the unreinforced status. In fact, reinforcement layers can treat the critical conditions of a foundation which is situated adjacent to the slope.
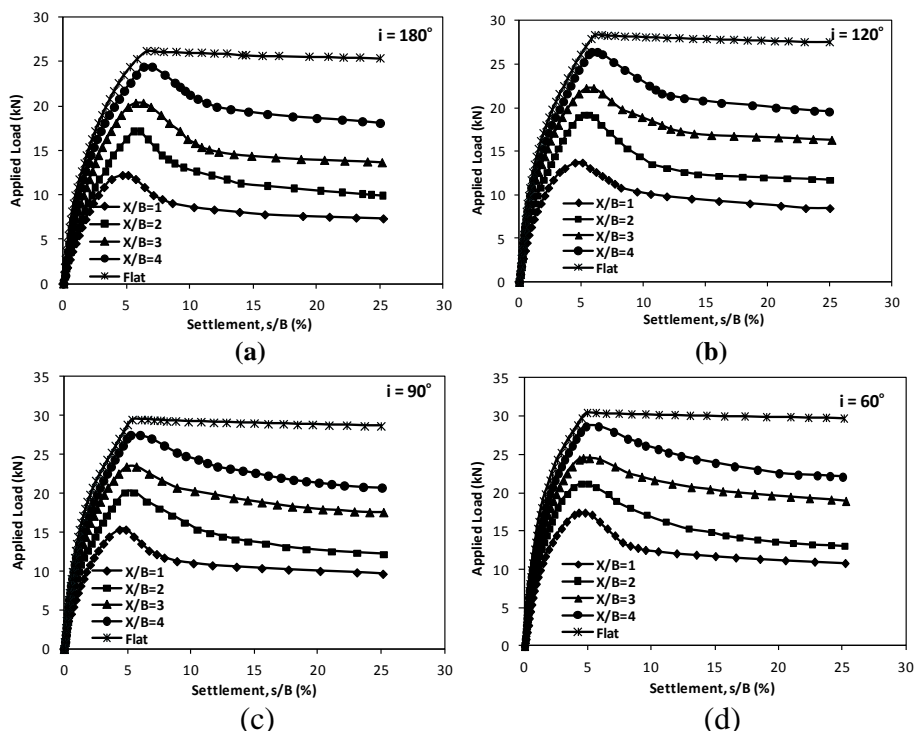
Figure 7. Load-settlement response of reinforced foundation on slope and flat backfills for (a) simple footing and shell footing with (b) i=120°, (c) i=90°, (d) i=60°.

To evaluate the failure mechanism of shell foundations located on reinforced slope, cracks and soil movements were visually captured during the tests. Also, at the end of each test, soil layer above the geotextiles was removed (see Figure 8) to investigate deformations of the reinforcement in terms of the length and depth of affected area over geotextiles.

Based on the visual inspection of reinforced tests, the following points can be concluded.

- According to Figure 9(a, b, c, d), the slope failure surface was progressed to second layer, continued parallel to this layer until crossed the slope face. It should be noted that Figs. 9(a) to 9(d) correspond to $x/B=1.0$. Although, cracks around the shell footings were not patently recognized; cracks in the backfill and at the end of geotextiles layers were visible with approximate width of 10mm. It was mentioned by other researchers that failure surface in reinforced slope crossed the slope's face around the second layer of reinforcements [19].

- Comparing the horizontal and vertical deformations of the affected area on the geotextiles (the right side of Figure 9), it is found out that penetration of shell footing into the sloped backfill, compared to the simple footing, resulted in stress distribution through the wider area. It can result to a larger failure zone accompanied by bearing capacity enhancement.

Parametric Study

The following sections explain the effects of reinforcement, edge distance and shell geometry on the ultimate bearing capacity and settlement of foundations. Moreover, some criteria for design and practice of shell footings, specifically located on slope backfills, have been specified.

Effect of Reinforcement

Figure 10 illustrates the effect of reinforcement on the response of shell footings. In this figure, bearing capacity ratio $(BCR)_u$,

according to Eq. (2), is defined as the ratio of bearing capacity of footings on the reinforced slope, $(Q)_{Re}$ to that of the unreinforced slope, $(Q)_{Ur}$ in a similar settlement ratio of 25%. Indeed, $(BCR)_u$ describes how much the performance of shell footing has been improved by the presence of reinforcement [33, 34].

$$(BCR)_u = \frac{(Q)_{Re}}{(Q)_{Ur}} \qquad (2)$$

According to Figure 10, reinforcement beneath shell footings can significantly improve the bearing capacity ratio of foundation in the range of 2.4 to 16, depending on the test conditions. In fact, geotextiles could successfully mobilize the anchorage potential, provided by pull-out resistance at the behind of sliding zone, resulted in stress reduction at depth and fortification of the affected area. It is obvious that the maximum bearing capacity ratio belonged to footings with the minimum edge distance due to the fact that not only the acquired bearing capacity of unreinforced foundation for shorter edge distance was small, but also, the effective length of geotextile behind the sliding zone is greater and results in mobilization of more pull-out resistance.

Based on Figure 10, it is evident that the rate of bearing capacity increment due to increasing apex angle is higher for x/B=1.0 compared to other values. On the other hand, the effectiveness of apex angle on the bearing capacity decreases when the footing gets away from the slope. For the flat ground, the effect of apex angle on the bearing capacity is negligible. This is due to the effect of apex angle on the depth of failure in shell foundations. Increase on apex
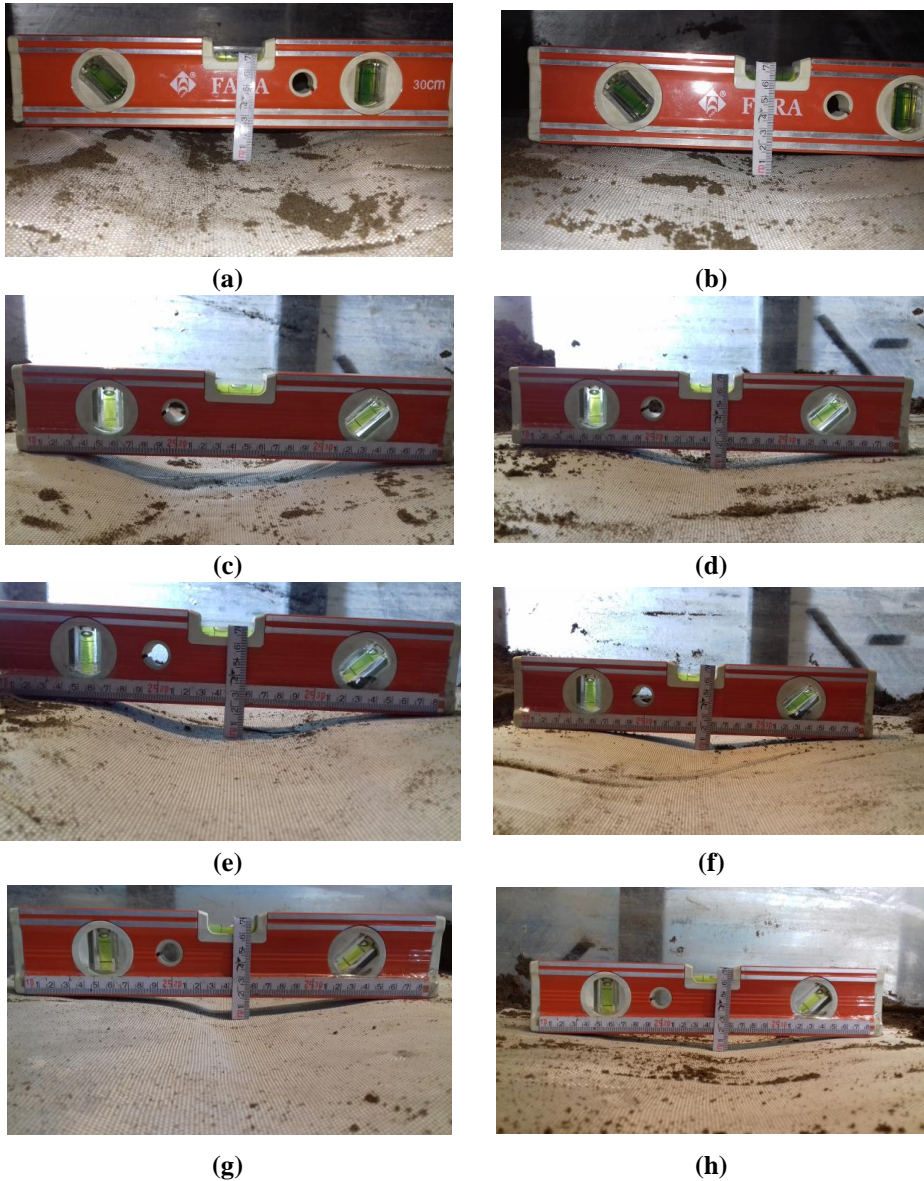
(a)

(b)

(c)

(d)

(e)

(f)

(g)

(h)

Figure 8. Deformation of geotextile layers beneath shell foundations (edge distance of 2B) on reinforced slope with apex angle (a, b) i=180°, (c, d) i=120°, (e, f) i=90° and (g, h) i=60° (left side for first layer and right side for second layer of the geotextiles)

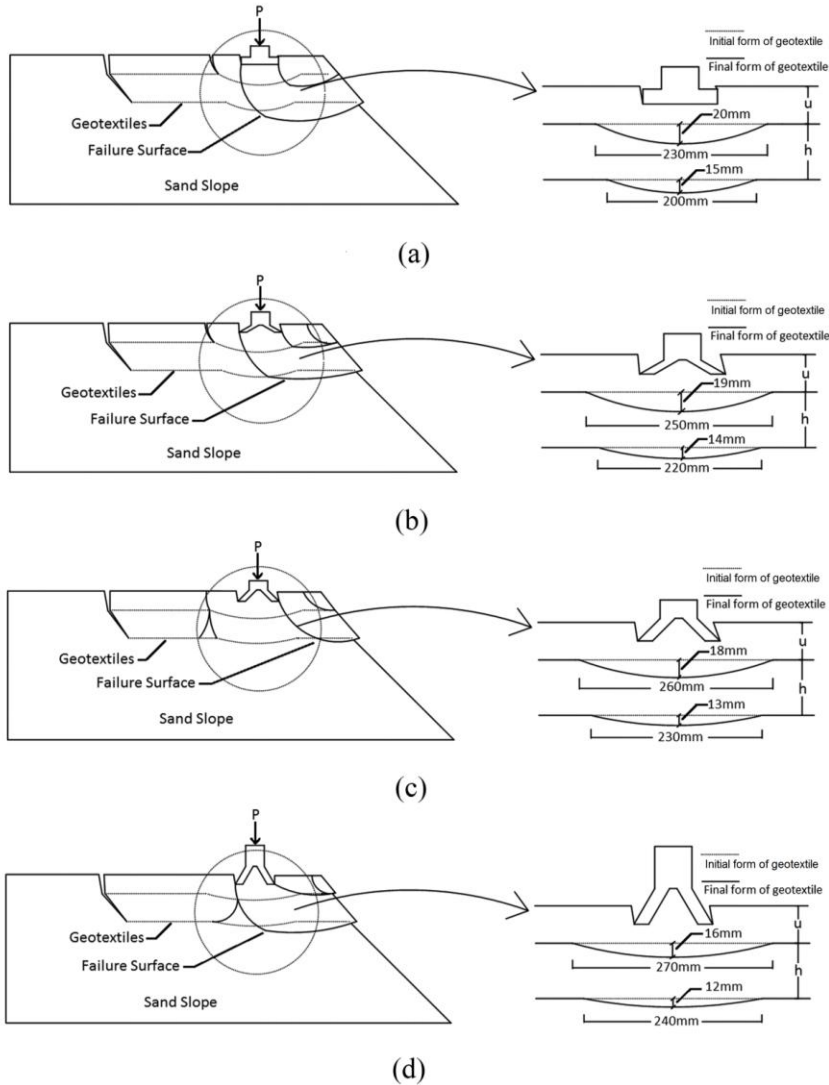**Figure 9. Failure mechanisms of shell foundations with apex angle (a) i=180°, (b) i=120°, (c) i=90° and (d) i=60° on reinforced slope for x/B=1.0 (left side for failure surfaces and right side for exerted deformations in geotextiles)**

angle decreases the failure depth which does not intersect the slope in greater edge distances.

Additionally, the results prove that decrease of apex angle tends to decrease the efficiency of reinforcement. It was previously described that contrary to the shell foundation performance, the reinforcement layers prevented stress distribution into the depth, tending to attenuate the shell foundation efficiency.
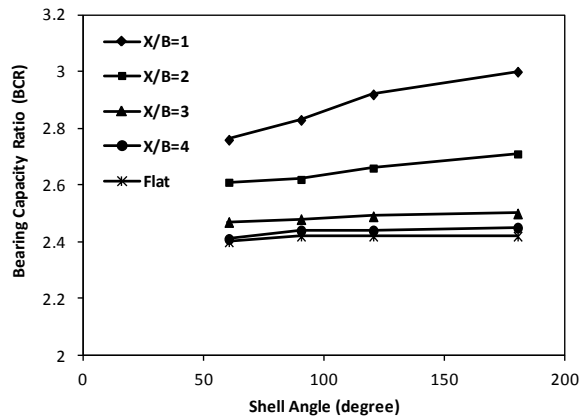

Figure 10. Bearing capacity ratio of foundations related to footings with respect to edge distance and apex angle

Influence of Apex Angle

To quantify how much the geometry of shell footing, in terms of apex angle, affects the bearing capacity of foundation in sloped and flat backfill, shell efficiency factor (SE) is defined according to Eq. (3). Herein, $(Q_u)_{sf}$ and $(Q_u)_{ff}$ are the ultimate bearing capacity of shell and simple footings, respectively.

$$(SE) = \frac{(Q_u)_{sf} - (Q_u)_{ff}}{(Q_u)_{ff}} \tag{3}$$

Based on the obtained results, variation of shell efficiency factor of all shell footings versus edge distance is depicted in Figure 11. It is obvious that shell footing with apex angle of 60° provides the most successful foundation system among the others. Conceivably, it was

happened based on the fact that the failure wedge of shell foundations, placed near to the slope crest, is formed deeper than the simple foundations which resulted in formation of considerably larger shear resistance zones.
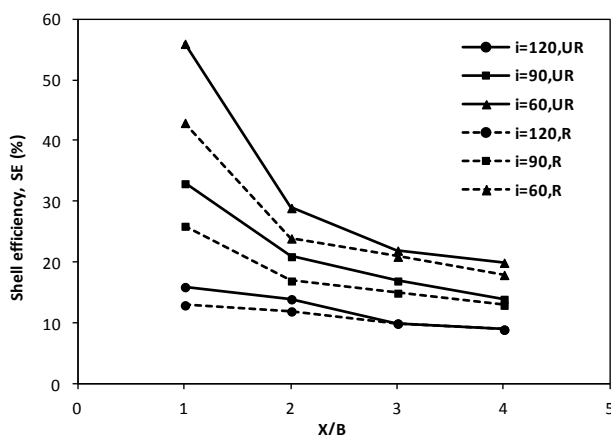
Figure 11. Shell efficiency factors of all shell footings located in unreinforced and reinforced statuses.

To have a better understanding of the shell efficiency, Figure 12 shows the failure wedge for different foundations in unreinforced status. Based on visual inspection, it is clear that the wedge angle of the failure surface has been increased as the apex angle became smaller. A decrease in apex angle from the flat one to 120°, 90° and 60°, increases the triangular wedge angle from 65° to 71°, 74° and 77°, respectively. This is an indicator of the deeper failure mode for shell foundations compared to flat ones. In the line with this observation, other researchers found out that the wedge of the failure surface of shell footing was deeper than that for simple footing due to the embedding effect [11].
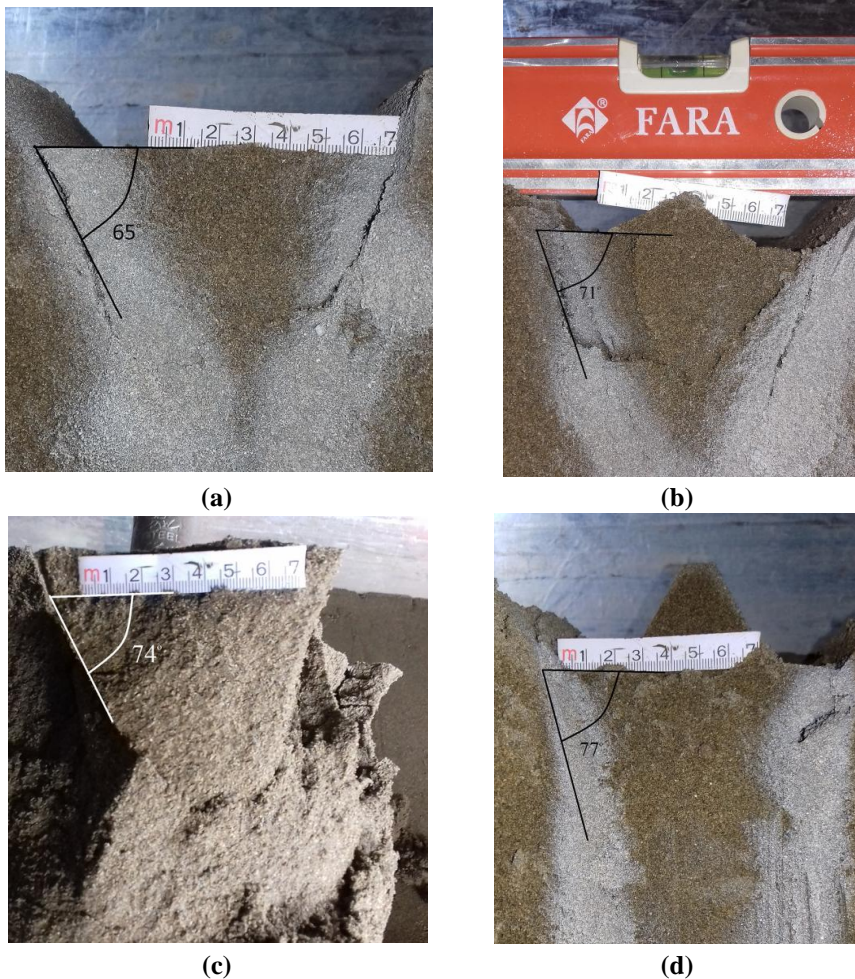
Figure 12. Photos of failure wedges for unreinforced shell foundations with (a) i= 180°, (b) i= 120°, (c) i= 90° and (d) i= 60°

To compare the formation of shear zones beneath the shell footings with different apex angles, Figure 13 is depicted. In this figure, the wedge failure angle (α) plays the main role in the efficiency of shell foundations. Equation (4) has been previously suggested for triangular shell strip footings to estimate wedge failure

angle (α). In this relationship, "SR" is called the shell ratio and φ is the soil's friction angle [35].

$$\alpha = \phi + (SR\text{-}1)\left(\frac{\pi}{4} - \frac{2\varphi}{3}\right) \tag{4}$$

SR is introduced according to Eq. (5) which represents the footing's configuration in the vertical direction. Here, θ equals to 90 − 0.5i, where "i" is the apex angle (see Figure 13).

$$SR = \frac{(\pi + 2\theta)}{\pi} \tag{5}$$

Based on the observations in the present study, Eq. (4) was verified and rewritten in the form of Eq. (6) for strip shell foundations.

$$\alpha = \left(\frac{\pi}{4} + \frac{\varphi}{2}\right) + (SR\text{-}1)\left(\frac{\pi}{4} - \frac{2\varphi}{3}\right) \tag{6}$$

Predominantly, as it can be seen in Figure 11, shell efficiency decreased due to the increase of edge distance. From this observation, it can be concluded that while shell footings are receded from the slope crest, the foundation response approaches (but never exactly the same) to the response of simple footing.

Hanna and Abd El-Rahman reported an experimental study on triangular shell foundations rested on flat sandy ground [36]. The apex angles were 180, 140, 100, 90 and 60 degrees. Table 6 shows a comparison between shell efficiency factors (as noted by SE in equation 3) that is determined from the results of present study for X=1B with that study. For an apex angle of 120 degrees, an average between the results for the apex angles of 140 and 100 degrees has been used.

According to the table, reduction of the apex angle from 180 to 60 degrees increased SE from zero to 43% based on the results of present study and from zero to 41% according to Hanna and Abd El-

Rahman [36]. Although the experiments of Hanna and Abd El-Rahman performed on unreinforced flat ground, there is a very good consistency with the results of present research.
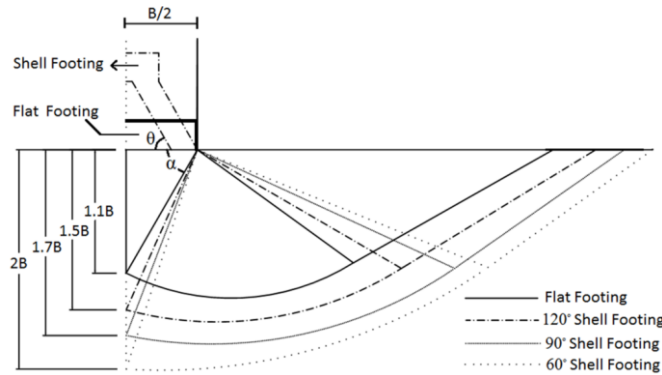
Figure 13. Schematic formation of shear zones in the shell foundations with different apex angles

Effect of Edge Distance

Once the footing is located on the slope, the bearing capacity is decreased because of removing a part of resistance zone adjacent to the slope. In order to investigate the bearing capacity variations, influenced by edge distance, a non-dimensional parameter namely "settlement factor (F_δ)" is introduced according to Eq. (7). Herein, "δ_u" is settlement at the ultimate bearing capacity, "γ" is soil unit weight, "A" is the area of the footing in horizontal projection and finally, "Q_u" defines ultimate bearing capacity. Since, the unit weight of the backfill was kept constant in all tests; a lower value of settlement factor indicates greater bearing capacity and represents better performance of foundation.

$$F_\delta = \frac{\delta_u \gamma A}{Q_u} \tag{7}$$

Figure 14 illustrates variations of settlement factor versus edge distance for all footings in either of reinforced and unreinforced conditions. Expectedly, irrespective of reinforcement status and apex angle, it is clear that as the footing gets closer to the slope, its settlement increases while the bearing capacity decreases which in turn, results in greater settlement factor. Also, increase in weight of moved soil which is approximately equal to $\delta_u \gamma A$ is greater for foundations near to the slope edge that results in decrease of the bearing capacity and increasing the settlement factor.

It should be mentioned that settlement factor varies in a small rate for edge distances more than 4B which implies the safe distance for footings rested on the sloped backfill.

Bearing Capacity Coefficient

The tested shell foundations are located on a sandy ground surface. As a result, the bearing capacity can be interpreted as follows:

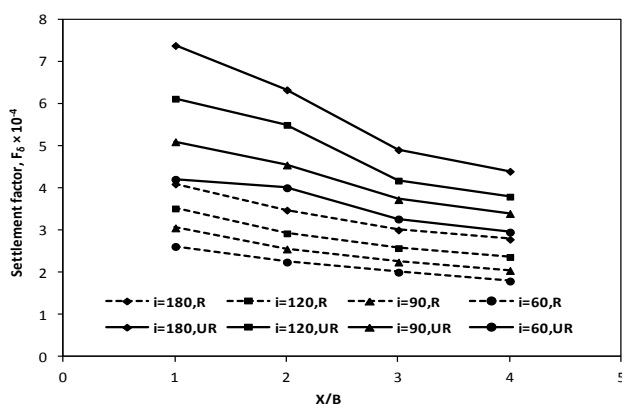$$q_u = \frac{1}{2} \gamma B N_\gamma'' \tag{8}$$

Figure 14. Variations of settlement factor versus edge distance for all footings in either of reinforced and unreinforced statuses

In this equation, N_γ'' shows the bearing capacity coefficient for shell foundation. Based on the values determined in experimental study, the bearing capacity coefficient is determined for shell foundation adjacent to the reinforced sandy slope. The concept for determination of this coefficient is the same as method implied at Attarzadeh et al. for flat footings near sandy slopes [37]. They proposed the following equation for flat footings near the unreinforced slopes:

$$\frac{N_\gamma'}{N_\gamma} = 0.159\left(\frac{X}{B}\right) + \left(-0.535\beta + 0.64\right) \tag{9}$$

In this equation, N_γ and N_γ' are the bearing capacity coefficients for the flat and sloped grounds and β is the slope angle in radians. The variables for reinforcement like the number of geotextile layers or distance between the first layer and bottom of foundation have not been considered in this study. So, equation (15) has also been used here for the footing adjacent to the reinforced slope considering the bearing capacity of footing located on reinforced flat ground at denominator. However, considering bearing capacity values for shell footings with different apex angles, the following equation is determined for the bearing capacity coefficient N_γ'' of the shell foundation adjacent to a reinforced sandy slope:

$$\frac{N_\gamma''}{N_\gamma'} = \left(0.058i - 0.137\right)\left(\frac{X}{B}\right) + \left(-0.296i + 1.762\right) \tag{10}$$

Here, i is the apex angle of shell foundation in radians.

Scale Effects

It should be certified that the presented experimental and empirical results are limited to one type of the backfill material with constant relative density and moisture constant, one type of geotextile with no variation in the number of layers and their geometries, constant slope angle and also, one type of footing material with constant embedded depth which are suggested for further studies in this field. As a result, specific applications should only be made after considering the above restrictions.

Also, any generalization on this subject necessitates the readers having studied the scale effect, vastly. Other researchers have considered the major physical parameters influencing the response of geogrid-reinforced slopes and used a dimensional analysis tending extrapolation towards the prototype case [19]. Based on their study, Eq. (17) can be suggested for the bearing capacity of shell foundations located on the geotextile-reinforced slopes.

$$Q_u = f(B. X. u. h. \beta. L. H. D_r. D_{50}. \varphi. c. \gamma. \vartheta. i. E_{soil}. E_{geo}. p_{shell}) \qquad (11)$$

where, D_r is the relative density of soil, D_{50} is the mean grain size, c is the cohesion intercept, ϑ is the Poisson's ratio, E_{soil} is the elasticity modulus of soil and E_{geo} is the elastic modulus of geotextile reinforcement. All other variables have been defined previously. Equation (11) can be represented in a non-dimensional form as Eq. (12):

$$\frac{Q_u}{\gamma AB} = f\left(\frac{X}{B}. \frac{u}{B}. \frac{h}{B}. \beta. \frac{L}{B}. \frac{H}{B}. D_r. \frac{D_{50}}{B}. \varphi. \frac{c}{\gamma B}. \frac{\gamma D_{50}}{E_{soil}}. \vartheta. i. \frac{E_{soil}}{E_{geo}}. \frac{p_{shell}}{\gamma B}\right) \qquad (12)$$

For the prototype shell footing with width (B_p) which is *n* times greater than that of the experimental model (B_m), Eq. (13) can be written:

$$\frac{B_p}{B_m} = n \tag{13}$$

As a result, when a prototype shell footing having the width of 1.2 m is considered, *n* will be 12; so considering equality of 15 non-dimensional variables in Eq. (18) for both prototype and model, the values of X, u, h, L, H and D_{50} should be considered 12 times of the model variables. Also, assuming the same unit weights for the soil used at model and prototype, values of c, E_{soil}, E_{geo} and p_{shell} should be considered 12 times of model parameters, as well. In this regard, the following equation can be considered between bearing capacities of the prototype $\left(\frac{Q_u}{A}\right)_p$ and model $\left(\frac{Q_u}{A}\right)_m$:

$$\left(\frac{Q_u}{\gamma AB}\right)_p = \left(\frac{Q_u}{\gamma AB}\right)_m \xrightarrow{so} \left(\frac{Q_u}{A}\right)_p = n \left(\frac{Q_u}{A}\right)_m \tag{14}$$

It should be noted that the proposed equations are based on the superposition law and are only valid at the elastic range of deformations at the soil and geotextile. To assess the scaling law for this system with higher accuracy, nonlinear behavior should be investigated. To do so, the stress portions for the both geotextile and soil should be determined based on consistency of deformations and then, the relevant equations could be derived.

Summary and Conclusion

In the present study, response of shell foundations situated near the edge of unreinforced and reinforced slopes was investigated and

compared with the conventional simple footings. To investigate the influence of different parameters such as shell footing's apex angle, reinforcement status and distance between footing and crest of the slope, on the bearing capacity and settlement, a comprehensive testing program was established. Based on the obtained results, the following conclusions can be drawn:

1. The maximum bearing capacity of shell foundations is higher than that of the conventional flat footings with the same dimensions in contact surface. For flat backfill, the bearing capacity of shell foundations was in the range of 8~18% more than the simple footing, depending on the apex angle. It might be due to the fact that the failure wedge in shell foundations is formed deeper than the simple footings which resulted in formation of considerably larger shear resistance zones.

2. The bearing capacity of shell foundations increased with decrease of apex angle. Compared to the simple footing, it increased in the range of 18 to 56% and 17 to 43%, for unreinforced and reinforced backfills, respectively.

3. The edge distance over the range of 4B is considered as safe distance for footings rested on the sloped backfill at which the ultimate bearing capacity approaches to that of flat condition.

4. The shell efficiency factor (SE), introduced to quantify increase in the ultimate bearing capacity of shell foundation in comparison to simple footing, increases with decrease of shell peak angle and decreases with increase of edge distance.

5. Existence of the reinforcement beneath shell footings could significantly improve the bearing capacity in the range of 2.4 to 3, depending on the test conditions. In fact, geotextiles could

successfully mobilize the anchorage potential, provided by pull-out resistance behind the sliding zone that results in more stabilization of the affected area.

6. Visual inspection of the rupture wedge surface in unreinforced tests and the movements of soil/reinforcement layers in reinforced tests revealed that shell footings extend the failure zone into the depth of foundation, tending to mobilize more resistance against footing penetration.

7. Contrary to the shell foundation system, the reinforcement layers prevent stress distribution into the depth of backfill, and expanded the rupture zone horizontally, instead. It resulted in debilitation of shell foundation efficiency.

References

1. Kurian N. P., Shah S. H., "Parametric studies on the ultimate strength of conical and spherical shell foundations", J Structural Engrg 12 (1985) 49-57.

2. Kurian N. P., "Shell foundations (Geometry, Analysis, Design and Construction)", Alpha Science International, Harrow, UK. (2006).

3. Yamamoto K., Lyamin A. V., Abbo A. J., et al, "Bearing capacity and failure mechanism of different types of foundations on sand", Soils and Foundations 42 (2009) 305-314.

4. Fernando N., Sendanayake E., Sendanayake D., et al, "The experimental investigation of failure mechanism and bearing capacity of different types of shallow foundations", Research Report, Department of Civil Engineering, University of Moratuwa, Sri Lanka (2011).

5. Kurian N. P., Mohan C. S., "Contact pressures under shell foundations. In: Proceedings of 10th international conference on soil mechanics and foundation engineering", Stockholm, Sweden (1981).

6. Esmaili D., Hataf N., "Experimental and numerical investigation of ultimate load capacity of shell foundation on reinforced and unreinforced sand", Iranian J Sci Tech 32 (2008) 491-500.

7. Thilakan S., Naik N., "Geotechnical behaviour of shell foundations. In: Proceedings of 50th Indian geotechnical conference", Pune, India (2015).

8. Hanna A., Abdel-Rahman M., "Maximum bearing capacity of triangular shell strip footings on sand", J Geotech Engrg 116 (1990) 1851-1863.

9. Hanna A., Abdel-Rahman M., "Experimental investigation of shell foundations on dry sand", Can Geotech J 35 (1998) 847-857.

10. Shaligram P. S., "Behavior of triangular shell strip footing on georeinforced layered sand", Int J Advanced Engrg Tech 2 (2011) 192-196.

11. Azzam W. R., Nasr A. M., "Bearing capacity of shell strip footing on reinforced sand", J Advanced Res 6 (2015) 727-737.

12. Lee K. M., Manjunath V. R., "Experimental and numerical studies of geosynthetic-reinforced sand slopes loaded with a footing", Can Geotech J 37 (2000) 828-842.

13. Viswanadham B. V. S., Konig D., "Studies on scaling and instrumentation of a geogrid", Geotex Geomem 22 (2004) 307-328.

14. El Sawwaf M., "Behavior of strip footing on geogrid-reinforced sand over a soft clay slope", Geotex Geomem 25 (2007) 50-60.

15. Alamshahi S., Hataf N., "Bearing capacity of strip footings on sand slopes reinforced with geogrid and grid-anchor", Geotex Geomem 27 (2009) 217-226.

16. Duangkhae S., Bergado D. T., Baral P., et al, "Analyses of reinforced embankment on soft and hard foundations", Ground Improvement 167 (2014) 3-23.

17. Artidteang S., Bergado D. T., Chaiyaput S., et al, "Embankment reinforced with limited life geotextiles on soft clay", Ground Improvement, 168 (2015) 130-143.

18. Rajabian A. B., Viswanadham B. V. S., "Behaviour of anchored geosynthetic- reinforced slopes subjected to seepage in a geotechnical centrifuge", Geosyn Int 23 (2016) 36-47.

19. Tavakoli Mehrjardi Gh., Ghanbari A., Mehdizadeh H., "Experimental study on the behaviour of geogrid-reinforced slopes with respect to aggregate size", Geotex Geomem 44 (2016) 862-871.

20. Vahidipour A., Ghanbari A., Hamidi A., "Experimental study of dynamic compaction adjacent to a slope", Ground Improvement, 169 (2016) 79-89.

21. Kazi M., Shukla S. K., Habibi D., "Behaviour of an embedded footing on geotextile-reinforced sand", Ground Improvement, 169 (2016) 120-133.

22. ASTM D 2487, "Standard practice for classification of soils for engineering purposes (Unified Soil Classification System)", ASTM Int, West Conshohocken, (2011) USA.

23. Selig E. T., Mc Kee K. E., "Static and dynamic behaviour of small footings", J Soil Mech Div 87 (1961) 29-47.

24. Chummer A. V., "Bearing capacity theory from experimental results", J Soil Mech Found Div 98 (1972) 1311-1324.

25. Dash S. K., Bora M. C., "Improved performance of soft clay foundations using stone columns and geocell-sand mattress", Geotex Geomem 41 (2013) 26-35.

26. ASTM D 4253, "Standard test methods for maximum index density and unit weight of soils using a vibratory table", ASTM Int, West Conshohocken, (2011) USA.

27. ASTM D 4254, "Standard test methods for minimum index density and unit weight of soils and calculation of relative density", ASTM Int, West Conshohocken, (2011) USA.

28. Sakti J. P., Das B. M., "Model tests for strip foundation on clay reinforced with geotextile layers", Transport Res Rec 1153 (1987) 40-45.

29. Chen Q., Abu-Farsakh M. Y., Sharma R., et al, "Laboratory investigation of behavior of foundations on geosynthetic-reinforced clayey soil", Transport Res Rec 2004 (2007) 28-38.

30. Abu-Farsakh M. Y., Chen Q., Yoon S., "Use of reinforced soil foundation (RSF) to support shallow foundation. Research Report", Louisiana Transportation Research Center, Louisiana, (2008) USA.

31. Altalhea E. B., Tahaa M. R., Abdrabbo F. M., "Bearing capacity of strip footing on sand slopes reinforced with geotextiles and soil nails", J Teknologi 65 (2013) 1-11.

32. Colmenares J. E., Kang S. R., Shin Y. J., et al, "Ultimate bearing capacity of conical shell foundation", Structural Engrg Mech 52 (2013) 507-523.

33. Badakhshan E., Noorzad A., "Load eccentricity effect on behavior of circular footing reinforced with geogrid sheets", J Rock Mech Geotech Engrg 7 (2017) 691-699.

34. Badakhshan E., Noorzad A., "Effect of footing shape and load eccentricity on behavior of geosynthetic reinforced sand bed", Geotex Geomem 45 (2017) 58-67.

35. Abdel-Rahman, M., "Geotechnical behavior of shell foundations", Dissertation, Concordia University (1996).

36. Hanna A., Abd El-Rahman M., "Ultimate bearing capacity of triangular shell strip footings on sand", J Geotech Engrg 116 (1990) 1851-1863.

37. Attarzadeh A., Ghanbari A., Hamidi A., "A study of bearing capacity of shallow foundations next to sand slope with experimental model", J Engrg Geol, Kharazmi University 9 (2015) 2695-2710.

Notations

u	embedded depth of the first reinforcement layer
h	distance between reinforcement layers
L	length of reinforcement
B	width of the shell footing
i	apex angle
$(BCD)_u$	bearing capacity decrease in unreinforced status
$(Q_u)_f$	bearing capacity in flat ground
$(Q_u)_s$	bearing capacity in sloped ground
X	edge distance to footing centerline
$(BCR)_u$	bearing capacity ratio
$(Q_u)_{Re}$	bearing capacity on reinforced slope
$(Q_u)_{Ur}$	bearing capacity on unreinforced slope
SE	shell efficiency
$(Q_u)_{sf}$	bearing capacity of shell footing
$(Q_u)_{ff}$	bearing capacity of simple footing
α	wedge failure angle
SR	shell ratio parameter
φ	Soil friction angle
θ	angle between shell's edge and ground
F_δ	settlement factor
δ_u	settlement at the ultimate bearing capacity
γ	soil unit weight
A	area of the footing in horizontal projection
Q_u	ultimate bearing capacity
N_γ	bearing capacity coefficient for footing on flat ground
N'_γ	bearing capacity coefficient for footing on sloped ground
N''_γ	bearing capacity coefficient for shell foundation on sloped ground
H	backfill height
β	backfill slope angle
W_f	weight of footing
D_r	relative density
D_{50}	mean grain size
c	cohesion intercept
ν	Poisson's ratio
E_{soil}	elasticity modulus of soil
E_{geo}	elasticity modulus of geotextile
B_p	width of prototype shell footing
B_m	width of model shell footing
n	size ratio of prototype and model footings

Table 1. Properties of Babolsar sand

Description	Value
Effective grain size, D_{10} (mm)	0.15
Medium grain size, D_{50} (mm)	0.25
Coefficient of uniformity, C_u	1.93
Coefficient of curvature, C_c	0.83
Specific gravity of solids, G_s	2.74
Maximum void ratio, e_{max}	0.80
Minimum void ratio, e_{min}	0.55
Water content (%)	4.5
Effective angle of internal friction, φ (degree)[*]	41
Cohesion intercept (kPa)[*]	0

[*]Obtained from consolidated-drained triaxial tests

Table 2. Mechanical properties of geotextile reinforcement

Parameter	Value
Tensile Strength MD[*] (kN/m)	100
Tensile Strength XMD[*] (kN/m)	50
Elongation MD/XMD (%)	10±2
Tensile Strength @ 5% Strain (MD) (kN/m)	50
Creep Reduced Strength (MD)-114 Years, 20°C (kN/m)	70.42

[*] MD: Machine Direction   XMD: Cross Machine Direction

Table 3. Testing program

Backfill Geometry	Reinforcement status	Apex angle (i, Degree)	Edge Distance (X)	Number of tests
Slope	Unreinforced Backfill	60, 90, 120, 180[*]	1B,2B,3B,4B	16
	Reinforced Backfill	60, 90, 120, 180[*]	1B,2B,3B,4B	16
Flat	Unreinforced Backfill	60, 90, 120, 180[*]	–	4
	Reinforced Backfill	60, 90, 120, 180[*]	–	4

[*] Shell footing with apex angle of 180° is known "simple footing" in this study.

Table 4. Values of ultimate bearing capacity and (BCD)u for different footings in unreinforced status

apex angle (Degree)	parameter	Edge distance in slope backfill (X)				
		1B	2B	3B	4B	Flat
180	Applied load at failure (kN)	4.06	6.32	8.12	9.93	10.83
	$(BCD)_u$ %	62	42	25	8	0
120	Applied load at failure (kN)	4.69	7.22	8.94	10.83	11.67
	$(BCD)_u$ %	60	38	24	8	0
90	Applied load at failure (kN)	5.42	7.67	9.48	11.28	12.18
	$(BCD)_u$ %	56	37	22	7	0
60	Applied load at failure (kN)	6.32	8.12	9.93	11.91	12.73
	$(BCD)_u$ %	50	36	22	6	0

Table 5. Values of ultimate bearing capacity and (BCD)u for different footings in reinforced status

apex angle (Degree)	Parameter	Edge distance in slope backfill (X)				
		1B	2B	3B	4B	Flat
180	Load at failure (kN)	12.18	17.15	20.31	24.37	26.17
	(BCD)$_u$ %	53	34	22	7	0
120	Load at failure (kN)	13.72	19.22	22.29	26.44	28.43
	(BCD)$_u$ %	52	32	22	7	0
90	Load at failure (kN)	15.34	20.13	23.47	27.53	29.51
	(BCD)$_u$ %	48	32	20	7	0
60	Load at failure (kN)	17.42	21.21	24.55	28.7	30.5
	(BCD)$_u$ %	43	30	20	6	0

Table 6. Comparison between shell efficiency factors of present study and Hanna and Abd El-Rahman [34]

Apex angle (Degrees)	SE (%) Current study (X=1B)	SE (%) Hanna and Abd El-Rahman [34]
180	0	0
120	13	18
90	26	30
60	43	41